Am J Physiol Cell Physiol 301: C938–C946, 2011.
First published July 13, 2010; doi:10.1152/ajpcell.00515.2010.

The $\alpha_7\beta_1$-integrin accelerates fiber hypertrophy and myogenesis following a single bout of eccentric exercise

Tara N. Lueders,[1,2] Kai Zou,[1,2] Heather D. Huntsman,[1,2] Benjamin Meador,[1] Ziad Mahmassani,[1,2] Megan Abel,[1,2] M. Carmen Valero,[1,2] Kimberly A. Huey,[3] and Marni D. Boppart[1,2]

[1]*Department of Kinesiology and Community Health and* [2]*Beckman Institute for Advanced Science and Technology, University of Illinois, Urbana, Illinois; and* [3]*College of Pharmacy and Health Sciences, Drake University, Des Moines, Iowa*

Submitted 21 December 2010; accepted in final form 6 July 2011

Lueders TN, Zou K, Huntsman HD, Meador B, Mahmassani Z, Abel M, Valero MC, Huey KA, Boppart MD. The $\alpha_7\beta_1$-integrin accelerates fiber hypertrophy and myogenesis following a single bout of eccentric exercise. *Am J Physiol Cell Physiol* 301: C938–C946, 2011. First published July 13, 2010; doi:10.1152/ajpcell.00515.2010.—The $\alpha_7\beta_1$-integrin is a heterodimeric transmembrane protein that adheres to laminin in the extracellular matrix, representing a critical link that maintains structure in skeletal muscle. In addition to preventing exercise-induced skeletal muscle injury, the α_7-integrin has been proposed to act as an intrinsic mechanosensor, initiating cellular growth in response to mechanical strain. The purpose of this study was to determine the extent to which the α_7-integrin regulates muscle hypertrophy following eccentric exercise. Wild-type (WT) and α_7-integrin transgenic (α_7Tg) mice completed a single bout of downhill running exercise ($-20°$, 17 m/min, 60 min), and gastrocnemius-soleus complexes were collected 1, 2, 4, and 7 days (D) postexercise (PE). Maximal isometric force was maintained and macrophage accumulation was suppressed in α_7Tg muscle 1D PE. Mean fiber cross-sectional area was unaltered in WT mice but increased 40% in α_7Tg mice 7D PE. In addition, a rapid and striking fivefold increase in embryonic myosin heavy chain-positive fibers appeared in α_7Tg mice 2D PE. Although Pax7-positive satellite cells were increased in α_7Tg muscle 1D PE, the number of nuclei per myofiber was not altered 7D PE. Phosphorylation of mammalian target of rapamycin (mTOR) was significantly elevated in α_7Tg 1D PE. This study provides the first demonstration that the presence of the $\alpha_7\beta_1$-integrin in skeletal muscle increases fiber hypertrophy and new fiber synthesis in the early time course following a single bout of eccentric exercise. Further studies are necessary to elucidate the precise mechanism by which the α_7-integrin can enhance muscle hypertrophy following exercise.

skeletal muscle; myogenesis; mammalian target of rapamycin

INTEGRINS ARE HETERODIMER glycoproteins composed of noncovalently bound α- and β-subunits that link extracellular matrix ligands with actin in the cytoskeleton (31). The $\alpha_7\beta_1$-integrin is highly expressed in skeletal muscle and appears to be critical for skeletal muscle development due to its presence in myoblasts during myogenesis, and it is equally important for maintaining structural integrity based on its expression in the sarcolemma, Z bands, and myotendinous (2) and neuromuscular (19) junctions in fibers. A vital role for the $\alpha_7\beta_1$-integrin in skeletal muscle is supported by genetic studies demonstrating that mutations in the α_7-gene (ITGA7) result in human congenital myopathies (14) and progressive muscular dystrophy in mice (20). Conversely, enhanced expression of the $\alpha_7\beta_1$-integrin in skeletal muscle of mice with a severe form of muscular dystrophy (*mdx/utr*$^{-/-}$) slows development of muscle pathology and markedly extends longevity (5, 6). Despite the known beneficial effect of the α_7-integrin in delaying neuromuscular disease symptoms, its mechanism of action remains elusive.

We have previously demonstrated that eccentric exercise increases α_7-integrin RNA transcripts, including both extracellular (X1 and X2) and intracellular (A and B) isoforms, in skeletal muscle 3 h postexercise (4). The α_4-,- α_5-, and α_6-integrin subunits are not upregulated, suggesting that the α_7-integrin is fulfilling a nonredundant, subunit-specific role within muscle following exercise. Concomitant increases in α_7B-integrin protein are observed 24 h exercise in whole muscle lysates, and immunofluorescence studies show enhanced localization of both A and B isoforms at myotendinous junctions (3, 4). Muscle creatine kinase (MCK)-driven expression of the α_7BX2-integrin (2- to 8-fold expression) effectively inhibits eccentric exercise-induced sarcolemmal injury, and this response is correlated with suppression of c-Jun NH_2-terminal kinase (JNK) activity (3). Conversely, skeletal muscle of α_7-integrin-null mice is susceptible to increased membrane damage following single or multiple bouts of eccentric exercise (4). These studies demonstrate that eccentric exercise initiates endogenous α_7-integrin synthesis and that integration of this molecule at the sarcolemma protects muscle from subsequent damage.

New fiber synthesis and/or increased growth of preexisting fibers via satellite cell fusion or increased protein synthesis is ultimately responsible for muscle hypertrophy observed following repeated eccentric contractions (9, 13, 22, 23). The extent to which each of these events contributes to whole muscle growth following exercise is still largely debated, but evidence exists to support both. Since the integrin represents a structure in skeletal muscle that has the ability to transmit mechanical force from the extracellular matrix to the actin cytoskeleton and vice versa, it has been proposed that the integrin may regulate exercise-induced skeletal muscle hypertrophy (12, 36). In an attempt to provide insight to this hypothesis, we previously evaluated the phosphorylation and activation of key hypertrophic signaling molecules, including Akt, mammalian target of rapamycin (mTOR), and p70 S6 kinase (p70S6K), in response to an acute bout of eccentric exercise in wild-type (WT) and α_7-integrin transgenic (α_7Tg) muscle (3). While phosphorylation of Akt, mTOR, and p70S6K was significantly increased (2-fold) in WT mice, activation was suppressed in α_7Tg mice, suggesting that hypertrophy might be inhibited in the transgenic mice postexercise. However, only early time points were measured postexercise (immediately and 3 h) and no other parameters of growth, including fiber

Address for reprint requests and other correspondence: M. D. Boppart, Beckman Institute for Advanced Science and Technology, 405 N. Mathews Ave., MC-251, Urbana, IL 61801 (e-mail: mboppart@illinois.edu).

cross-sectional area (CSA) or satellite cell number, were assessed in the days following acute exercise in this study.

Satellite cells, muscle stem cells located between the sarcolemma and basal lamina surrounding individual muscle fibers, are essential for muscle development but become mitotically quiescent during adulthood, fulfilling a sporadic role in muscle repair and hypertrophy following injury (29). When activated by a variety of muscle-, vessel-, and inflammatory cell-derived growth factors in response to injury, satellite cells upregulate the expression of Pax7 and myogenic markers (Myf-5 and myoD) and subsequently enter the cell cycle (24, 33, 37). The transition from cell proliferation to terminal differentiation requires the inhibition of cell division and upregulation of myogenin, Myf-4, and the embryonic form of myosin heavy chain (eMHC) (8, 13, 26). Satellite cells are activated in response to acute and chronic weight-bearing exercise in rodents and humans (13, 30) and can directly engraft and repair injured muscle fibers from a central location in the fiber and/or fuse with other satellite cells to support de novo fiber synthesis postexercise (1, 11).

Satellite cell accumulation and fiber hypertrophy have been observed in skeletal muscle of 10-wk-old *mdx/utr*$^{-/-}$ mice overexpressing the α_7-integrin (7). In addition, satellite cell activation is deficient in $\alpha_7^{-/-}$ mice following cardiotoxin injury (27). The fact that the α_7BX2-integrin may regulate the proliferation and/or appearance of satellite cells in muscle prompted us to reevaluate the influence of the α_7-integrin on postexercise hypertrophy. The α_7-integrin transgenic mouse model resistant to muscle damage also provides a unique opportunity to determine whether mechanical strain can facilitate muscle growth in an injury-independent manner in vivo.

The purpose of this study was to test the hypothesis that the α_7-integrin is a regulator of exercise-induced skeletal muscle hypertrophy. Muscle growth was assessed by measuring individual fiber and whole muscle cross-sectional areas and new fiber synthesis. In addition, the contribution of Pax7-positive (Pax7$^+$) satellite cells and mTOR signaling to muscle growth was evaluated.

METHODS

Animals. Protocols for animal use were approved by the Institutional Animal Care and Use Committee of the University of Illinois at Urbana-Champaign (UIUC). α_7Tg mice (SJL/C57BL6: MCK-α7BX2) were produced at the University of Illinois Transgenic Animal Facility as described (3, 5). α_7Tg mice used for this study express eightfold higher levels of α_7-integrin protein compared with WT mice (3). All experiments were conducted at approximately the same time of day. Animals were fed standard laboratory chow and had access to water ad libitum. Five- or eight-week-old female WT and α_7Tg mice remained at rest (basal conditions) or completed a single downhill running exercise ($-20°$, 17 m/min, 60 min). Speed on the treadmill (Exer-6M, Columbus Instruments, Columbus, OH) was gradually increased from 10 to 17 m/min during a 7-min warm-up period (increase of 1 m/min every minute). A subset of mice [n = 2/group (grp); WT and α_7Tg, basal and 1 day postexercise (1D PE)] were injected intraperitoneally with Evan's blue dye (0.5 mg/ml, 0.05 ml/10 g body wt) 90 min before exercise to verify membrane damage as previously reported (3, 4). Mice were euthanized via carbon dioxide asphyxiation 1, 2, 4, and 7 days postexercise (2D–7D PE, $n \geq$ 5/grp; 1D PE, n = 4–5/grp). Sedentary WT and α_7Tg basal controls were euthanized at 5 wk and 4 days of age. Basal control mice were euthanized at 9 wk for force measurements and 5 wk for assessment of macrophage content.

Contractile force measurements. Functional testing was completed to detect post-eccentric exercise injury in WT and α_7Tg mice. Maximal isometric force of the plantarflexors was measured in situ as previously described (21) for each of the following groups: WT basal, α_7Tg basal, WT 7D PE, and α_7Tg 7D PE (n = 5/grp). The force-measurement apparatus consisted of a servomotor and analog control unit (model 305C-LR, Aurora Scientific, Aurora, ON, Canada), a square-wave stimulator (model 2100, A-M Systems, Carlsborg, WA), and a PC running a customized LabView 8.2 program controlling the servomotor and stimulator. For force measurements, mice were anesthetized by the intraperitoneal administration of 100 mg/kg ketamine, 10 mg/kg before the sciatic nerve was stimulated at 250 Hz for 1.5 s to evoke a maximal contraction. The values of force output (g) were normalized to muscle weight (g/g muscle weight). Mice used for functional measures were not used for further histological assessments.

Processing of muscle for histology. Gastrocnemius-soleus complexes were rapidly dissected and frozen in precooled isopentane. It is standard procedure in our laboratory to dissect the gastrocnemius and soleus muscles as a complex, rather than as separate muscles, because of the relatively small size of the soleus in our control mice that do not express the α_7-integrin (not used in this study). Muscles were embedded in optimal cutting temperature compound (Tissue-Tek; Fisher Scientific, Hanover Park, IL), and 8–10 μm cryosections were cut distally from the center (3 sections per sample, separated by ~100 μm) using a CM1850 cryostat (Leica, Wezlar, Germany). Sections were placed on microscope slides (Superfrost; Fisher Scientific) and stored at $-80°$C before staining.

Evaluation of fiber and whole muscle CSA. To delineate fibers for area measures, membranes were outlined by immunostaining for the α_7-integrin. Frozen sections were fixed in acetone for 5 min and blocked with PBS containing 5% bovine serum albumin (BSA). The rat α_7B-integrin cytoplasmic domain was detected with the use of purified α_7CDB polyclonal rabbit anti-rat antibody (CDB 1:500) (32). For all histological assessments, species-appropriate secondary antibodies were applied at 1:100–1:200 (Jackson ImmunoResearch Laboratories, West Grove, PA). Following staining, slides were mounted using Vectashield containing DAPI nuclear stain (Vector Laboratories, Burlingame, CA) and examined with a Leica DMRXA2 microscope. Images were acquired using a Zeiss AxioCam digital camera and OpenLab software (Zeiss, Thornwood, NY). Fiber cross-sectional areas were measured using the advanced measurements component of Axiovision software on images obtained with a $\times$20 objective. Mean fiber CSA was obtained by measuring the areas of 1,000 fibers from each animal in the basal state and 7D PE (n = 4/grp). For all histological assessments described in this study, investigators were blinded to sample information.

For evaluation of whole muscle hypertrophy, images were obtained using a $\times$5 objective. Because of the large size of the muscle cross sections from the center of the gastrocnemius, 10–20 images were obtained from each section and reconstructed into a single image with Adobe Photoshop, using transparency settings to overlay the images using morphological markers. The mean whole muscle CSA was then calculated for three sections/animal using Axiovision software.

Evaluation of new fiber synthesis. Newly synthesized fibers were detected by expression of eMHC in muscle cross sections and the presence of nuclei in the central location within muscle fibers. Sections were fixed in acetone for 5 min, blocked with 1$\times$ PBS containing 10% horse serum, blocked with 70 μg/ml goat anti-mouse monovalent Fab fragments [AffiniPure Fab Fragment Goat Anti-Mouse IgG (H+L), Jackson ImmunoResearch Laboratories] diluted in 10% horse serum, and incubated with mouse monoclonal 47A (1:10) antibody (kindly provided by Peter Merrifield, University of Western Ontario, Canada) for 1 h. Total eMHC-positive (eMHC$^+$) fibers were

counted in 40 fields of view using a ×20 objective (3 sections/sample; $n \geq 6$/grp).

Hematoxylin and eosin staining for assessment of centrally located nuclei (CLN) in separate samples was completed with an automated robotic slide stainer (Leica Autostainer XL, Leica Instrument, Nussloch, Germany). Nuclei localization was evaluated in a total of 1,000 fibers per animal (≥6 mice/grp) using a ×20 objective.

Assessment of mononuclear cells and myonuclear number. Macrophage appearance was assessed with rat anti-F4/80 antibody (1:100) (AbD Serotec, Raleigh, NC), and satellite cells were detected with Pax7 antibody (1:2) (Developmental Studies Hybridoma Bank, Iowa City, IA) using methods described for eMHC, except that 5% BSA was used for blocking and Pax7 antibody was applied overnight. The total number of macrophages was counted in a total of 50 fields using a ×40 objective ($n = 4$/grp). Total $Pax7^+$ fibers were counted in 40 fields using a ×40 objective ($n \geq 6$/grp).

To delineate fibers for assessment of myonuclear content, membranes were identified by immunostaining for dystrophin (1:100) (MANDRA1, Sigma). Frozen sections were fixed in acetone for 10 min and blocked with PBS containing 5% BSA and blocked with 70 μg/ml goat anti-mouse monovalent Fab fragments diluted in 1% BSA. Nuclei were identified by using DAPI, incorporated in the Vectashield mounting media. Merged dystrophin and DAPI images were obtained using a ×40 objective, and an Adobe Photoshop counting tool was used to manually assess the number of nuclei in 200 fibers per animal ($n = 6$/grp). Nuclei were considered myonuclei only if clearly located on the inside of the dystrophin border.

Evaluation of mTOR phosphorylation. Frozen gastrocnemius-soleus complexes from WT and α7TG mice were manually ground with a porcelain mortar and pestle chilled in liquid nitrogen. Powdered tissue was homogenized in 10 volumes of an ice-cold buffer containing 20 mM HEPES (pH = 7.4), 2 mM EGTA, 50 mM β-glycerophosphate, 1 mM dithiothreitol, 1 mM Na_3VO_4, 1% Triton X-100, and 10% glycerol, supplemented with 10 μM leupeptin, 3 mM benzamidine, 5 μM pepstatin A, 1 mM phenylmethylsulfonyl fluoride, and 10 μg/ml aprotinin. The homogenates were rotated at 4°C for 1 h and centrifuged at 14,000 *g* for 15 min at 4°C, and supernatant was removed as the detergent-soluble fraction. Protein concentration was determined with the Bradford protein assay using BSA for the standard curve.

Equal amounts of protein (60 μg) were separated by SDS-PAGE using 8% acrylamide gels and transferred to nitrocellulose membranes. Equal protein loading was verified by Ponceau S staining. Membranes were blocked in Tris-buffered saline (pH 7.8) containing 8% BSA, and membranes were incubated with phospho-mTOR antibody overnight (1:1,000) and subsequently reprobed for total mTOR (Cell Signaling Technology, Danvers, MA). Horseradish peroxidase-conjugated anti-rabbit secondary antibodies (Jackson ImmunoResearch) were applied for 1 h. Bands were detected using Pierce enhanced chemiluminescence Western blotting substrate (Thermo Scientific, Rockford, IL) and a Bio-Rad ChemiDoc XRS system (Bio-Rad, Hercules, CA).

Localization of activated mTOR was detected in muscle using an antibody that detects phosphorylation of mTOR on serine 2448 (Cell Signaling Technology). Sections were fixed in 4% paraformaldehyde for 10 min, permeabilized with 0.25% Triton X-100 for 10 min, blocked with 5% BSA for 30 min, and incubated with primary antibody (1:50) overnight at 4°C.

Statistical analysis. All averaged data are presented as means ± SE. Comparisons between WT and α7Tg mice, basal and exercised, were performed by two-way ANOVA to determine whether an interaction effect was observed for group and time. Tukey post hoc analysis was performed when appropriate main or interaction effects were found for eMHC, CLN, mean fiber CSA, and Pax7 data (SigmaStat). Least-significant difference (LSD) post hoc analysis was performed on macrophage content, myonuclear number per fiber, and phospho-mTOR data (version 16, SPSS). Unpaired *t*-tests were completed to detect differences in maximal isometric forces and fiber CSA distribution (SigmaStat). For all tests, differences were considered significant at $P < 0.05$.

RESULTS

α7-Integrin transgenic mice are protected from functional deficits postexercise. We previously established that skeletal muscle overexpressing the α7-integrin is protected from sarcolemmal damage (3). In this study, preservation of membrane damage was verified by Evan's blue dye staining of muscle sections (Fig. 1*A*). In addition, we measured maximal isometric force in WT and α7Tg muscle 7D PE (Fig. 1*B*). At baseline, muscle force was similar between WT (216.3 ± 11.2) and α7Tg mice (213.6 ± 10.7) (Fig. 1*B*). At 7D PE, a deficit in

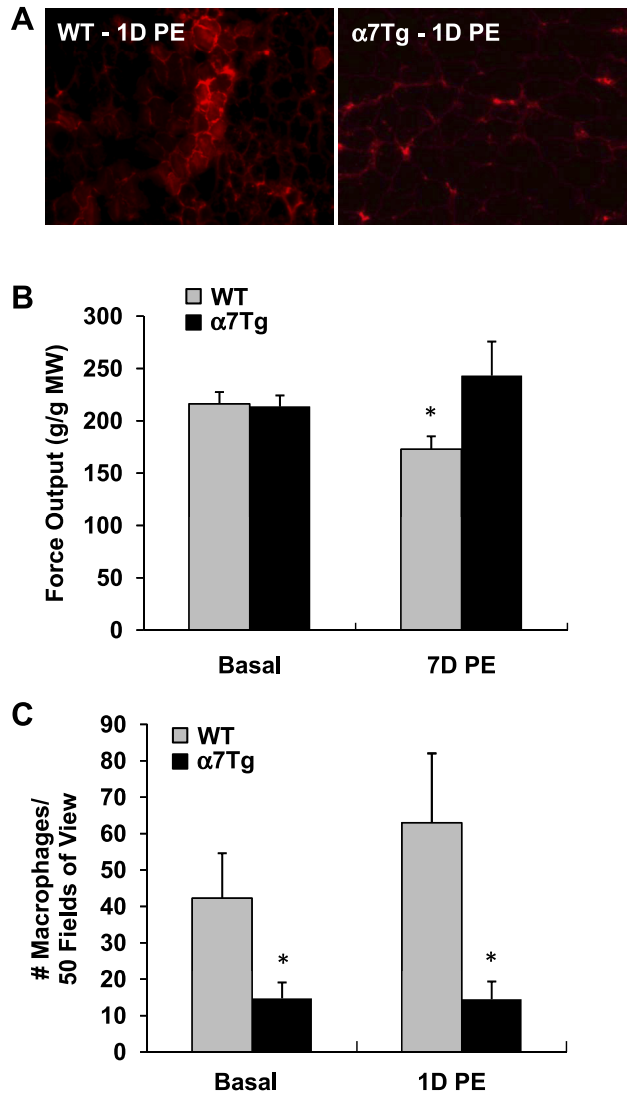

Fig. 1. Exercise-induced injury is prevented and macrophage accumulation is suppressed in α7-integrin transgenic (α7Tg) mice following exercise. *A*: Evan's blue dye was visualized in wild-type (WT; *left*) and α7Tg (*right*) muscle 1 day (D) postexercise (PE). *B*: maximal isometric contraction strength of hindlimb plantarflexors was measured in situ via stimulation of the sciatic nerve under anesthesia in the basal (nonexercised) state and 7D PE. MW, muscle weight. *C*: macrophages were detected by expression of F4/80 using immunodetection methods in cross sections of WT and α7Tg muscle in the basal state and 1D PE. *$P < 0.05$ vs. basal WT.

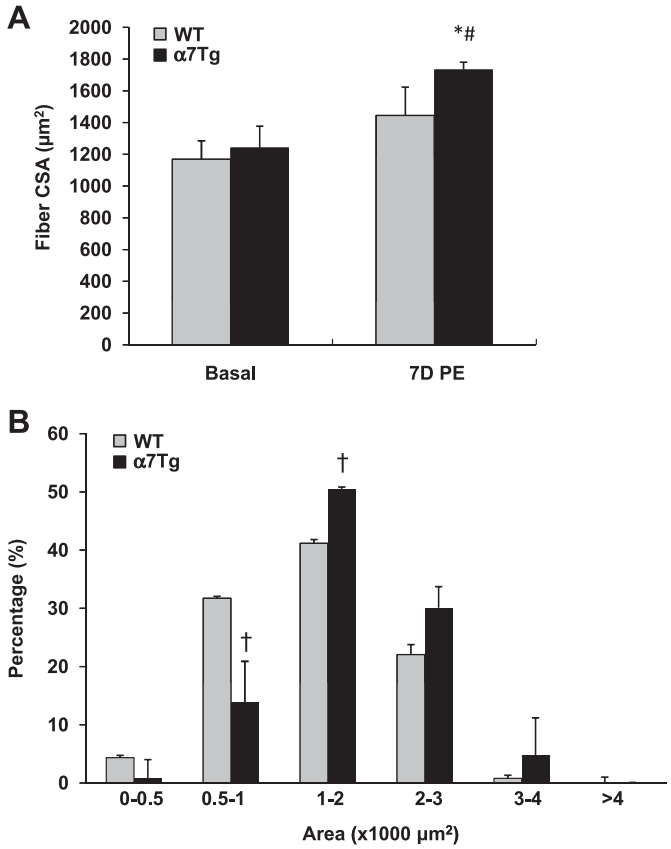

Fig. 2. Fiber cross-sectional area (CSA) is increased in α_7Tg mice 7 days postexercise. Fiber CSA was measured in 1,000 fibers from WT and α_7Tg mice 7D PE. *A*: mean CSA for each group was determined after averaging the area of all fibers in each animal. *B*: distribution of fiber sizes in WT and α_7Tg mice 7D PE. *$P < 0.05$ vs. basal WT; #$P < 0.05$ vs. basal α_7Tg; †$P < 0.05$ vs. 7D WT.

force was observed in WT mice compared with baseline (172.9 ± 12.4) ($P < 0.05$). In contrast, α_7Tg mice were protected from declines in postexercise force (243.1 ± 32.6). Consistent with these results, macrophage content was suppressed in α_7Tg both in the basal state and 1D PE compared with WT mice that did not exercise ($P < 0.05$; Fig. 1*C*).

Enlargement of muscle fibers in α7Tg mice postexercise. The cross-sectional areas of individual muscle fibers were measured in WT and α_7Tg mice in the basal state and 7D PE (Fig. 2, *A* and *B*). A significant increase in mean fiber CSA was not detected in exercised compared with nonexercised WT mice. However, a 40% increase in CSA was observed in α_7Tg mice 7D PE compared with α_7Tg mice that did not exercise (1,242.3 ± 135.2 basal vs. 1,733.7 ± 46.9 7D PE) ($P < 0.05$; Fig. 2*A*). Further analysis of the fiber CSA distribution postexercise revealed a significant decrease in 500–1,000 μm² and an increase in 1,000–2,000 μm² fibers in α_7Tg muscle compared with WT ($P < 0.05$; Fig. 2*B*).

Myogenesis is accelerated in α7Tg skeletal muscle following exercise. To determine whether the α_7Tg positively regulates new fiber formation postexercise, we analyzed fibers for eMHC expression and the presence of centrally located nuclei in both WT and α_7Tg mice. Small-caliber, triangular-shaped eMHC$^+$ fibers with hyperchromatic and enlarged central nuclei were detected in WT and α_7Tg mice in the days following a single bout of downhill running exercise compared with nonexercised controls (Fig. 3*A*). A rapid 5.2-fold increase in the total number of eMHC$^+$ fibers was detected in α_7Tg mice 2D PE (66.94 ± 16.2) compared with α_7Tg mice that did not exercise (12.89 ± 3.43) ($P < 0.001$; Fig. 3*B*), whereas the number of eMHC$^+$ fibers remained unaltered in WT mice. At 4D PE, new fiber development remained significantly elevated (4.5-fold; $P < 0.001$) in α_7Tg. The number of eMHC$^+$ fibers was no longer significantly elevated at 7D PE, and eMHC

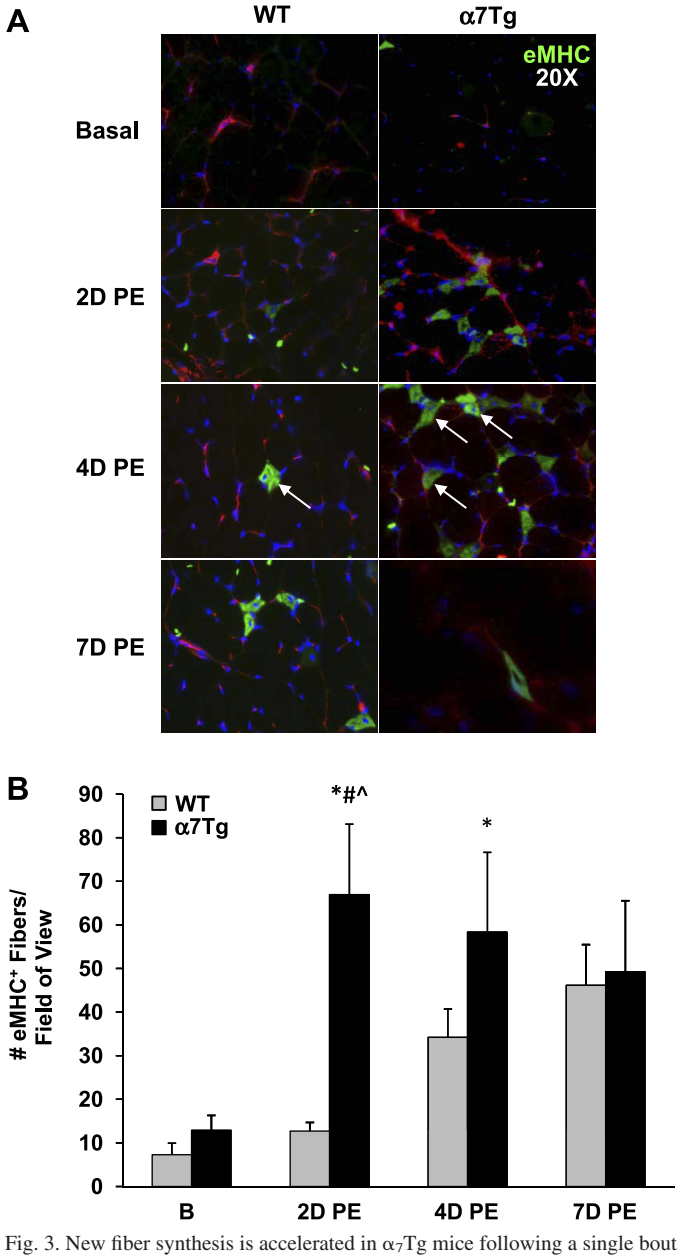

Fig. 3. New fiber synthesis is accelerated in α_7Tg mice following a single bout of eccentric exercise. Newly generated fibers were detected by expression of embryonic myosin heavy chain (eMHC) and small-caliber, triangular-shaped morphology (arrows) in muscle cross sections of WT and α_7Tg muscle in the basal (nonexercised) state (denoted B) or 2, 4, and 7 days postexercise. *A*: representative immunostaining of eMHC-positive (eMHC$^+$) fibers (eMHC = green fluorescence). *B*: total number of eMHC$^+$ fibers was quantitated by counting fibers in 40 fields of view at ×20 magnification. *$P < 0.001$ vs. basal WT; #$P < 0.001$ vs. basal α_7Tg; ^$P < 0.001$ vs. 2D PE WT.

staining was never observed in large-caliber fibers in WT or α_7Tg muscle.

Newly synthesized fibers incorporate a single nuclei in the central position of the fiber, purportedly to allow for a smaller myonuclear domain size and efficient synthesis of newly translated myofibrillar proteins (28). Therefore, identification of CLN in the fiber provides an alternative method for evaluation of new fiber generation (10). The rate of appearance of CLN correlated with eMHC expression. As shown in Fig. 4*B*, a 5.3-fold increase in CLN was observed in α_7Tg mice at 2D PE (77.83 ± 13.04) compared with α_7Tg mice that did not exercise (14.56 ± 1.85) ($P < 0.001$). By two-way ANOVA, an interaction effect was observed between group and time. Whereas most CLN$^+$ fibers were small caliber at 2D PE and located adjacent to other CLN$^+$ fibers in clusters, most CLN$^+$ fibers were large caliber and isolated by 7D PE (Fig. 4*A*).

A single bout of eccentric exercise does not acutely increase whole muscle weight or CSA. Absolute gastrocnemius muscle weight (Fig. 5*A*) or relative to body weight (not shown) was not different between WT and α_7Tg mice in the basal state or 7D PE. In addition, whole muscle CSA was not increased in response to a single bout of exercise at this early time point postexercise (Fig. 5*B*).

Satellite cells are elevated but do not contribute to increased myonuclear number per fiber postexercise. To determine the basis for increased fiber hypertrophy and myogenesis, we next examined satellite cell accumulation, myonuclear content per fiber, and activation of mTOR phosphorylation. In agreement with other studies examining the satellite cell response to exercise, the number of Pax7$^+$ cells increased 67% in WT muscle 2D PE ($P < 0.05$; Fig. 6*A*). However, Pax7$^+$ cells peaked earlier, increasing 81% 1D PE, in α_7Tg muscle compared with WT muscle in the nonexercised state (not significant vs. α_7Tg basal; $P < 0.05$ vs. WT basal). Despite the significant increase in Pax7$^+$ cells in both WT and α_7Tg mice, the myonuclear number per fiber remained unaltered at 7D PE (Fig. 6*B*).

mTOR phosphorylation is increased in α7Tg muscle following exercise. mTOR is a serine/threonine protein kinase that regulates protein synthesis in mammalian cells. The proportion of activated mTOR (phospho-mTOR: mTOR ratio) was found to be significantly elevated 1D PE ($P < 0.05$ vs. α_7Tg basal; Fig. 7*A*), just before the peak in eMHC$^+$ cells 2D PE. No differences in mTOR phosphorylation were detected in WT mice postexercise. Active mTOR in α_7Tg muscle cryosections was localized to the sarcolemma and cytoplasm of mature fibers, with intense staining around select nuclei inside or outside the fibers, consistent with previous findings (15) (Fig. 7*B*).

DISCUSSION

We previously reported that the α_7-integrin is upregulated in response to injury or strain associated with a single bout of eccentric exercise (3, 4). Muscle-specific transgenic expression of the α_7-integrin protects muscle fibers from damage following eccentric exercise in healthy WT mice and increases the number of regenerative satellite cells in muscle, the fusion of these stem cells into muscle fibers during repair, and fiber hypertrophy in dystrophic mice (3, 4, 7). However, a role for the α_7-integrin in eccentric exercise-induced hypertrophy re-

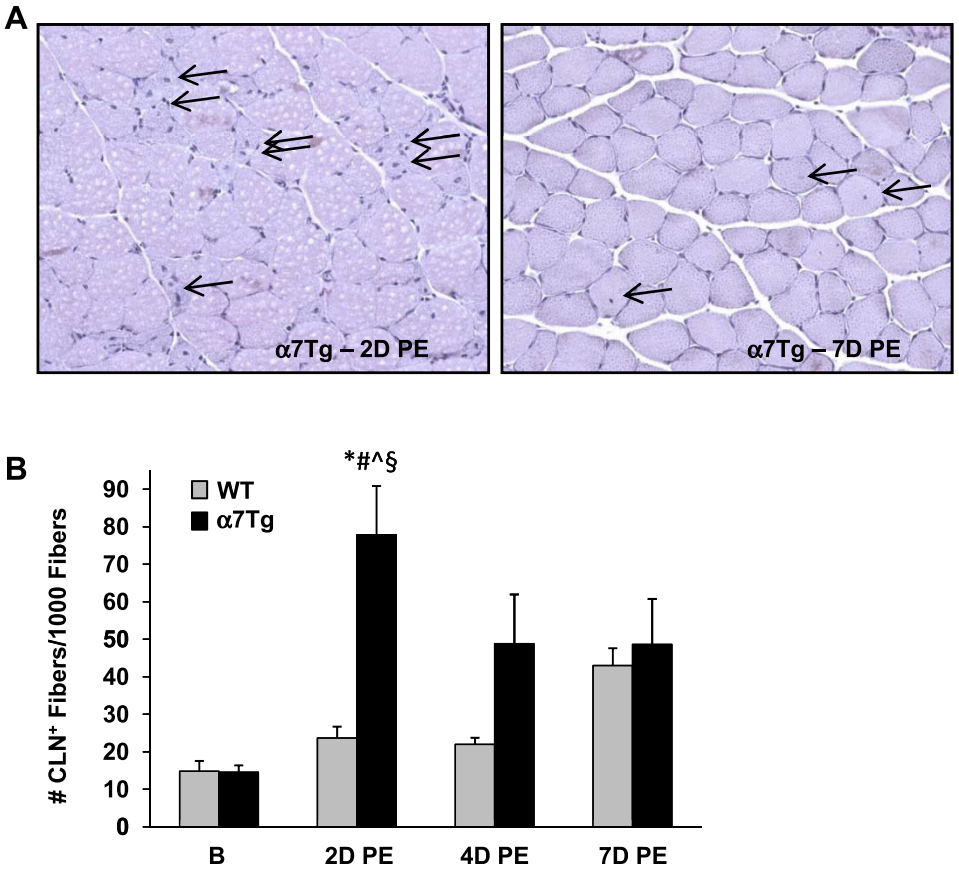

Fig. 4. Small-caliber fibers with centrally located nuclei (CLN) are increased in α_7Tg mice following a single bout of eccentric exercise. Newly generated fibers were detected by the presence of CLN in small-caliber fibers. *A*: representative histology showing clusters of small-caliber fibers with CLN 2D PE (arrows) and isolated large-caliber fibers with CLN 7D PE (arrows) in cross sections of α_7Tg skeletal muscle. *B*: total number of CLN$^+$ fibers was quantitated by assessing the presence of nuclei in the central position in a total of 1,000 fibers per animal. *$P < 0.001$ vs. basal WT; #$P < 0.001$ vs. basal α_7Tg; ^$P < 0.001$ vs. 2D PE WT; §$P < 0.001$ vs. 4D PE WT.

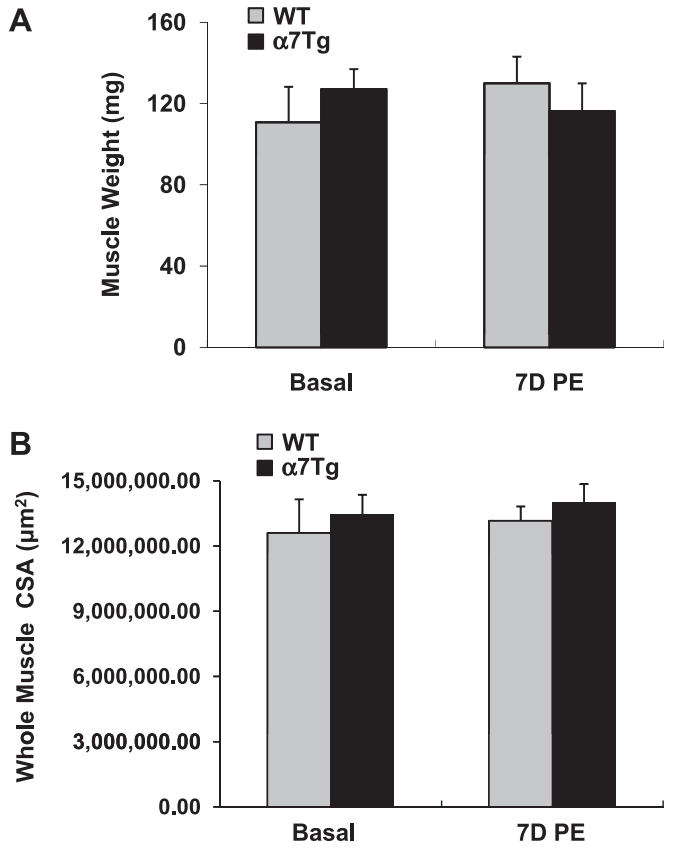

Fig. 5. Whole muscle weight and CSA are not altered following a single bout of eccentric exercise. *A*: gastrocnemius-soleus complex weight was measured (in mg). *B*: mean whole CSA for each group was determined after averaging the CSA of three sections for each animal.

mains to be established. This study provides the first demonstration that exercise-induced muscle growth is accelerated with elevated expression of the α_7-integrin.

The α_7-integrin is a transmembrane protein that has been hypothesized to facilitate eccentric exercise-mediated hypertrophy due to its ability to integrate mechanical forces across the sarcolemma (12, 36). We previously reported suppression of Akt, mTOR, and p70S6K phosphorylation in α_7Tg skeletal muscle immediately and/or 3 h following a single bout of eccentric exercise compared with WT skeletal muscle (3). However, in the current study, the mean fiber CSA was increased 40% 7D PE in α_7Tg muscle compared with α_7Tg muscle that was not exposed to the acute bout of exercise. The distribution of fiber sizes revealed a significant drop in the percentage of small (500–1,000 μm) fibers and a concomitant increase in the percentage of larger fibers in α_7Tg muscle 7D PE. The rapid increase in fiber size was somewhat surprising given the acute stimulus provided. Since the increase in fiber CSA could be explained by either satellite cell fusion or enhancement of protein synthesis, we evaluated $Pax7^+$ cells, myonuclear number per fiber, and the activation and localization of mTOR. Although $Pax7^+$ cells were significantly increased in α_7Tg muscle 1D PE, the myonuclear number per fiber was not altered at 7D PE, suggesting that satellite cell fusion was not responsible for the increase in fiber hypertrophy. However, mTOR activation was increased at 1D PE, with mTOR phosphorylation predominantly concentrated in the sarcolemma of mature fibers. These results suggest that the α_7-integrin may directly facilitate growth of skeletal muscle in response to acute mechanical stimulation via activation of hypertrophic signaling. Additional in vitro experiments are needed to determine whether the α_7-integrin can directly influence the hypertrophic signaling response and growth of primary myotubes derived from WT, α_7Tg, and $\alpha_7^{-/-}$ mice. In addition, the hypertrophic response to repeated bouts of eccentric exercise should be investigated in future studies.

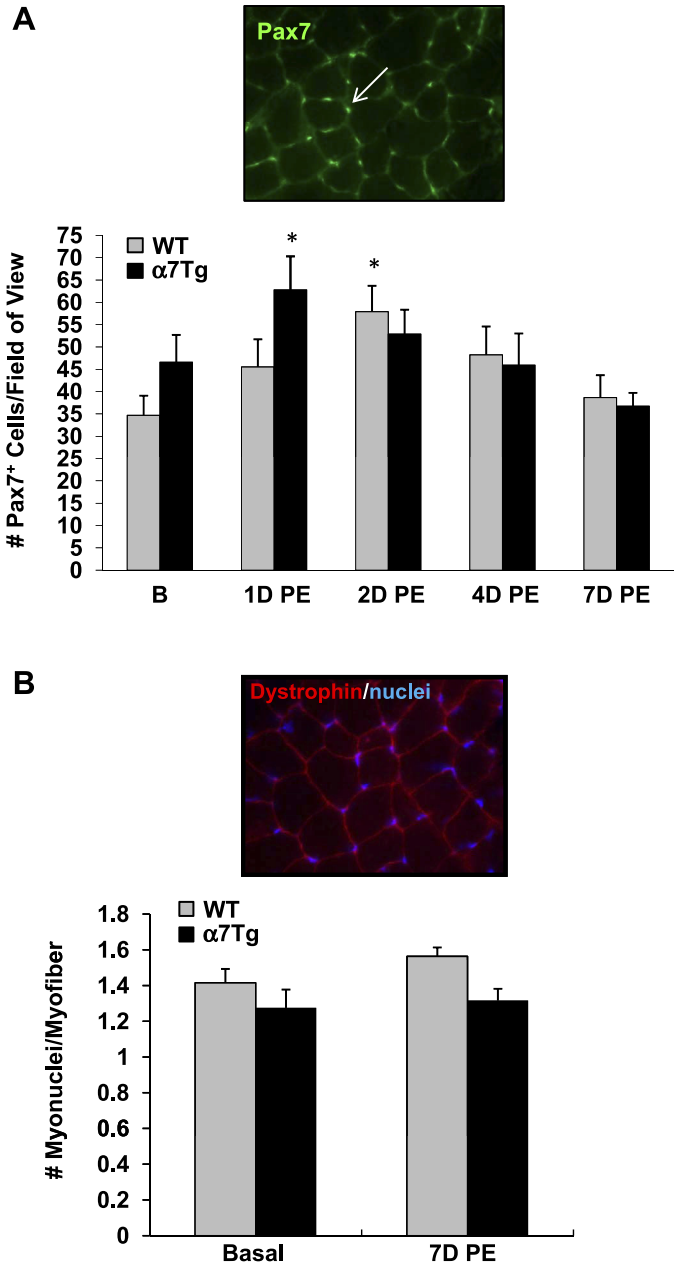

Fig. 6. Satellite cells are enhanced but do not fuse with existing fibers following a single bout of eccentric exercise. *A*: quiescent and activated satellite cells were identified by expression of Pax7 (arrow) using immunodetection methods in cross sections of WT and α_7Tg muscle in the basal (nonexercised) state and 1, 2, 4, and 7 days postexercise (Pax7 = green fluorescence). Total number of $Pax7^+$ cells was quantitated by counting cells in 40 fields of view at ×40 magnification. *B*: average number of nuclei inside each fiber at 7D PE was measured in 200 fibers/animal (dystrophin = red fluorescence, nuclei = blue fluorescence). $^*P < 0.05$ vs. basal WT.

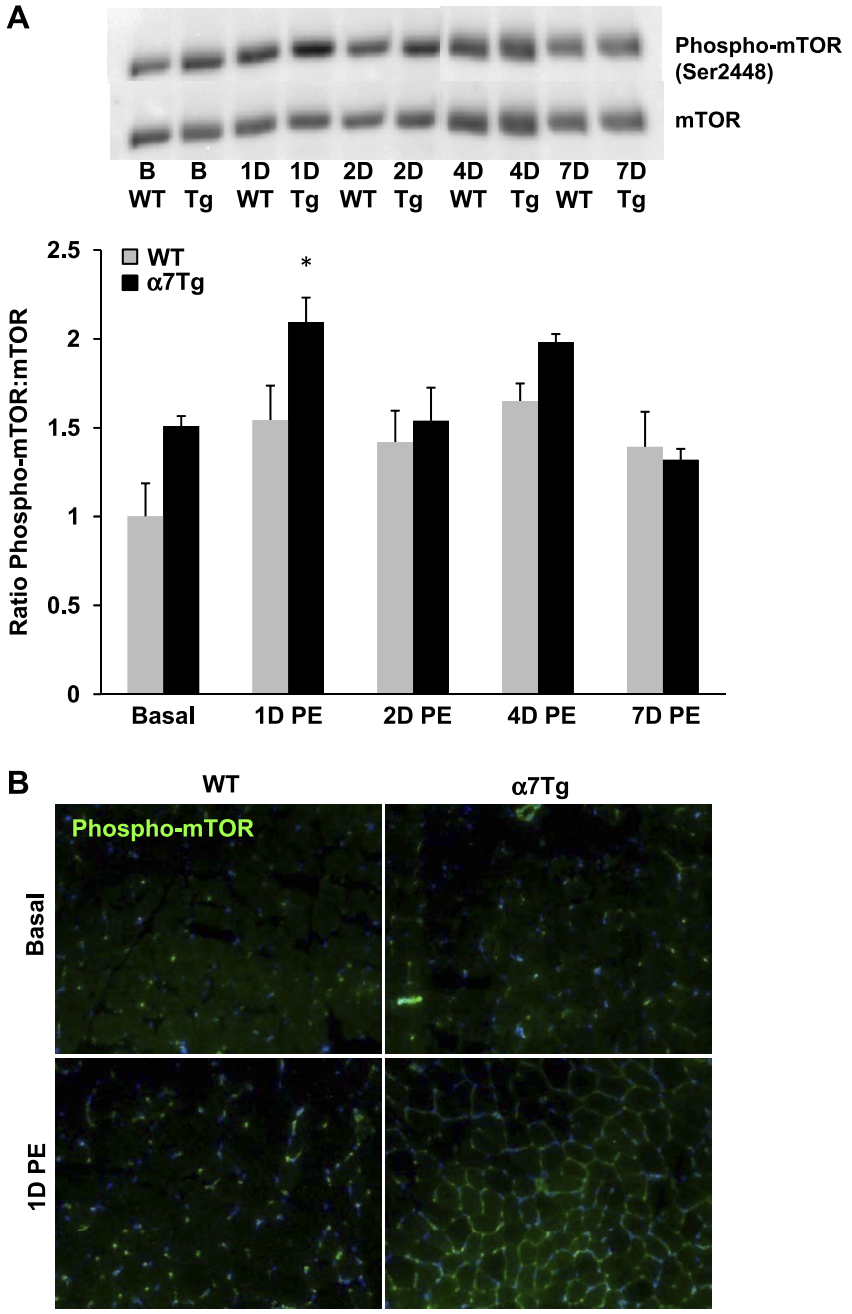

Fig. 7. Mammalian target of rapamycin (mTOR) phosphorylation is increased in α_7Tg mice following exercise. *A*: the proportion of active mTOR was detected by immunoblotting in WT and α_7Tg muscle in the basal (nonexercise) state and 1, 2, 4, and 7 days postexercise. *B*: representative immunostaining of phospho-mTOR in WT and α_7Tg muscle in the basal state and 1D PE (phospho-mTOR = green fluorescence, nuclei = blue fluorescence). *$P < 0.05$ vs. basal α_7Tg.

A marked increase in new fiber synthesis was also observed in α_7Tg mice subjected to a single bout of downhill running exercise. Whereas small, triangular shaped eMHC$^+$ fibers with enlarged CLN rapidly appeared in α_7Tg muscle at 2 days, a more gradual insignificant rise in the presence of these fibers was observed in WT mice in the days following exercise. We noted an increase in the size and a concomitant decrease in fluorescence intensity in eMHC$^+$ fibers from 2D to 7D PE in α_7Tg mice, likely reflecting transition to expression of the adult myosin heavy chain isoform (28). Verification of new fiber maturation was obtained from the CLN data since this parameter should theoretically be maintained during the 7-day period. In α_7Tg muscle, fibers with CLN were predominantly small 2D PE, whereas fibers with CLN were larger by 7D PE (Fig. 4*A*). In both α_7Tg and WT muscle, small eMHC$^+$ fibers with CLN were clustered 2D PE, whereas larger CLN$^+$ fibers were isolated and distanced from one another 7D PE. We noted a tendency for nuclei in the central location to migrate toward the periphery in isolated CLN$^+$ fibers 7D PE (Fig. 4*A*). Therefore, we speculate that clusters of CLN$^+$ fibers no longer existed at 7D PE due to the rapid maturation of newly formed fibers. Alternatively, newly developed fibers may undergo apoptosis; however, this is unlikely given the role of the α_7-integrin in protection from apoptosis in healthy and dystrophic mice (5, 17). Postexercise myogenesis observed in this study is in agreement with human studies that demonstrate increases in eMHC$^+$ cells in biopsies of skeletal muscle following both endurance and resistance exercise (16).

Downhill running has been used as a physiological, noninvasive model for the induction of satellite cells in rodent and human skeletal muscle which potentially contribute to postexercise adaptations and growth, including new fiber synthesis (1, 18, 25, 35). In this study, we observed a 60% increase in satellite cell number at 2D PE and a concomitant increase in $eMHC^+$ fibers at 7D PE in WT mice. In contrast, satellite cell numbers were elevated as early as 1D PE and new fibers were present in significant numbers 2D PE in α_7Tg mice. The observations suggest that the α_7-integrin could have indirectly and directly contributed to new fiber synthesis. First, it is possible that increased adherence and decreased postexercise injury provided by the α_7-integrin established a microenvironment conducive to satellite cell proliferation and/or fusion. Second, the α_7-integrin transgene expressed in satellite cells may have contributed to rapid differentiation of these myogenic progenitor cells, directly contributing to accelerated fiber synthesis. In addition, we cannot rule out the possibility that the α_7-integrin can facilitate the release of growth factors (IGF-I) from skeletal muscle that might increase the proliferation and fusion of satellite cells for increased new fiber synthesis. Further studies are necessary to substantiate a role for the α_7-integrin in one or a combination of these events postexercise.

We did not anticipate the dramatic adaptations in skeletal muscle provided by the α_7-integrin following eccentric exercise. Although the increase in mean fiber CSA and new fiber synthesis in α_7Tg muscle had the potential to increase absolute muscle weight, relative muscle weight, and whole muscle hypertrophy, we did not observe any of these changes at 7 days following an acute bout of eccentric exercise. We believe that the early changes in α_7Tg muscle, though appreciated on a microscale, were not significant enough to be assessed on a larger scale. Repeated bouts of exercise are commonly required to induce changes in whole muscle weight and size. In addition, unlike the synergistic ablation model and other models of strain-induced hypertrophy, downhill running includes an endurance component that might alter tissue composition. The application of the synergistic ablation model and repeated mechanical load to the α_7Tg mouse model is the most logical measure towards elucidating the full extent to which the integrin regulates exercise-induced hypertrophy.

The predominant finding of this paper is the increase in muscle growth with overexpression of the α_7-integrin postexercise. We also verify the lack of muscle injury previously observed in these mice using functional and immunological measures. A single bout of eccentric exercise can disrupt structures within the excitation-contraction coupling complex and induce ultrastructural damage within Z bands, resulting in significant deficits in the ability to generate force for several weeks (35). In this study, a decrease in force was observed in WT mice 7D PE, reflective of muscle injury. In contrast, muscle force was preserved in α_7Tg mice. The lack of macrophage content in α_7Tg skeletal muscle is consistent with these findings and suggests that the α_7-integrin may indirectly suppress exercise-induced skeletal muscle inflammation. To our knowledge, this is the first in vivo study to suggest that mechanical strain may be sufficient for skeletal muscle growth and that neither injury nor the presence of macrophages are necessary for this process.

In conclusion, this study demonstrates that the α_7Tg-integrin is an important regulator of early hypertrophic growth of skeletal muscle in response to eccentric exercise. Further work should be carried out using both in vivo and in vitro experiments to elucidate the predominant mechanism by which the α_7-integrin facilitates fiber hypertrophy and new fiber synthesis following exercise.

ACKNOWLEDGMENTS

We thank Jordan Orr and Dr. Nadia Nasreen for technical assistance. We also thank Dr. Derek Milner for donating Pax7 antibody.

GRANTS

This work was supported by grants from the Illinois Regenerative Medicine Institute, Ellison Medical Foundation, Mary Jane Neer Foundation (UIUC), and Arnold O. Beckman Award (UIUC) (to M. D. Boppart).

DISCLOSURES

No conflicts of interest, financial or otherwise, are declared by the author(s).

REFERENCES

1. **Armand AS, Launay T, Della Gaspera B, Charbonnier F, Gallien CL, Chanoine C.** Effects of eccentric treadmill running on mouse soleus: degeneration/regeneration studied with Myf-5 and MyoD probes. *Acta Physiol Scand* 179: 75–84, 2003.
2. **Bao ZZ, Lakonishok M, Kaufman S, Horwitz AF.** $\alpha 7\beta 1$ integrin is a component of the myotendinous junction in skeletal muscle. *J Cell Sci* 106: 579–590, 1993.
3. **Boppart MD, Burkin DJ, Kaufman SJ.** $\alpha_7\beta_1$-Integrin regulates mechanotransduction and prevents skeletal muscle injury. *Am J Physiol Cell Physiol* 290: C1660–C1665, 2006.
4. **Boppart MD, Volker SE, Alexander N, Burkin DJ, Kaufman SJ.** Exercise promotes $\alpha 7$ integrin gene transcription and protection of skeletal muscle. *Am J Physiol Regul Integr Comp Physiol* 295: R1623–R1630, 2008.
5. **Boppart MD, Burkin DJ, Kaufman SJ.** Activation of AKT signaling promotes cell growth and survival in $\alpha 7\beta 1$ integrin-mediated alleviation of muscular dystrophy. *Biochim Biophys Acta* 1812: 439–446, 2011.
6. **Burkin DJ, Wallace GQ, Nicol KJ, Kaufman DJ, Kaufman SJ.** Enhanced expression of the $\alpha 7\beta 1$ integrin reduces muscular dystrophy and restores viability in dystrophic mice. *J Cell Biol* 152: 1207–1218, 2001.
7. **Burkin DJ, Wallace GQ, Milner DJ, Chaney EJ, Mulligan JA, Kaufman SJ.** Transgenic expression of the $\alpha 7\beta 1$ integrin maintains muscle integrity, increases regenerative capacity, promotes hypertrophy, and reduces cardiomyopathy in dystrophic mice. *Am J Pathol* 166: 253–263, 2005.
8. **Butler-Browne GS, Whalen RG.** Myosin isozyme transitions occurring during the postnatal development of the rat soleus muscle. *Dev Biol* 102: 324–334, 1984.
9. **Bruusgaard JC, Johansen IB, Egner IM, Rana ZA, Gundersen K.** Myonuclei acquired by overload exercise precede hypertrophy and are not lost on detraining. *Proc Natl Acad Sci USA* 107: 15111–15116, 2010.
10. **Carosio S, Berardinelli MG, Aucello M, Musaro A.** Impact of ageing on muscle cell regeneration. *Ageing Res Rev* 10: 35–42, 2009.
11. **Crameri RM, Langberg H, Magnusson P, Jensen CH, Schroder HD, Olesen JL, Suetta C, Teisner B, Kjaer M.** Changes in satellite cells in human skeletal muscle after a single bout of high intensity exercise. *J Physiol* 558: 333–340, 2004.
12. **Durieux AC, D'Antona G, Desplanches D, Freyssenet D, Klossner S, Bottinelli R, Fluck M.** Focal adhesion kinase is a load-dependent governor of the slow contractile and oxidative muscle phenotype. *J Physiol* 587: 3703–3717, 2009.
13. **Hawke TJ, Garry DJ.** Myogenic satellite cells: physiology to molecular biology. *J Appl Physiol* 91: 534–551, 2001.
14. **Hayashi YK, Chou FL, Engvall E, Ogawa M, Matsuda C, Hirabayashi S, Yokochi K, Ziober BL, Kramer RH, Kaufman SJ, Ozawa E, Goto Y, Nonaka I, Tsukahara T, Wang JZ, Hoffman EP, Arahata K.** Mutations in the integrin alpha7 gene cause congenital myopathy. *Nat Genet* 19: 94–97, 1998.

15. **Hulmi JJ, Tannerstedt J, Selanne H, Kainulainen H, Kovanen V, Mero AA.** Resistance exercise with whey protein ingestion affects mTOR signaling pathway and myostatin in men. *J Appl Physiol* 106: 1720–1729, 2009.
16. **Kadi F, Thornell LE.** Training affects myosin heavy chain phenotype in the trapezius muscle of women. *Histochem Cell Biol* 112: 73–78, 1999.
17. **Liu J, Burkin DJ, Kaufman SJ.** Increasing $\alpha_7\beta_1$-integrin promotes muscle cell proliferation, adhesion, and resistance to apoptosis without changing gene expression. *Am J Physiol Cell Physiol* 294: C627–C640, 2008.
18. **Malm C, Sjodin TL, Sjoberg B, Lenkei R, Renstrom P, Lundberg IE, Ekblom B.** Leukocytes, cytokines, growth factors, and hormones in human skeletal muscle and blood after uphill or downhill running. *J Physiol* 556: 983–1000, 2004.
19. **Martin PT, Kaufman SJ, Kramer RH, Sanes JR.** Synaptic integrins: selective association of the α1 and α7A, and α7B subunits with the neuromuscular junction. *Dev Biol* 174: 125–139, 1996.
20. **Mayer U.** Integrins: redundant or important players in skeletal muscle? *J Biol Chem* 278: 14587–14590, 2003.
21. **Meador B, Huey KA.** Glutamine preserves skeletal muscle force during an inflammatory insult. *Muscle Nerve* 40: 1000–1007, 2009.
22. **Miyazaki M, Esser KA.** Cellular mechanisms regulating protein synthesis and skeletal muscle hypertrophy in animals. *J Appl Physiol* 106: 1367–1373, 2009.
23. **O'Connor RS, Pavlath GK.** Point:Counterpoint: Satellite cell addition is/is not obligatory for skeletal muscle hypertrophy. *J Appl Physiol* 103: 1099–1100, 2007.
24. **Parise G, O'Reilly CE, Rudnicki MA.** Molecular regulation of myogenic progenitor populations. *Appl Physiol Nutr Metab* 31: 773–781, 2006.
25. **Parise G, McKinnell IW, Rudnicki MA.** Muscle satellite cell and atypical myogenic progenitor response following exercise. *Muscle Nerve* 37: 611–619, 2008.
26. **Rhodes SJ, Konieczny SF.** Identification of MRF4: a new member of the muscle regulatory factor gene family. *Genes Dev* 3: 2050–2061, 1989.
27. **Rooney J, Gurpur PB, Yablonka-Reuveni Z, Burkin D.** Laminin-111 restores regenerative capacity in a mouse model for α7 integrin congenital myopathy. *Am J Pathol* 174: 256–264, 2009.
28. **Rosser BW, Dean MS, Bandman E.** Myonuclear domain size varies along the lengths of maturing skeletal muscle fibers. *Int J Dev Biol* 46: 747–754, 2002.
29. **Sambasivan R, Tajbakhsh S.** Skeletal muscle stem cell birth and properties. *Semin Cell Dev Biol* 18: 870–882, 2007.
30. **Snijders T, Verdijk LB, van Loon LJC.** The impact of sarcopenia and exercise training on skeletal muscle satellite cells. *Ageing Res Rev* 8: 328–338, 2009.
31. **Song WK, Wang W, Foster RF, Bielser DA, Kaufman SJ.** H36-α7 is a novel integrin α-chain that is developmentally regulated during skeletal muscle myogenesis. *J Cell Biol* 117: 643–667, 1992.
32. **Song WK, Wang W, Sato H, Bielser DA, Kaufman SJ.** Expression of α7 integrin cytoplasmic domains during skeletal muscle development: alternate forms, conformational change, and homologies with serine/threonine kinases and tyrosine phosphatases. *J Cell Sci* 106: 1139–1152, 1993.
33. **Tidball JG, Wehling-Henricks M.** Macrophages promote muscle membrane repair and muscle fibre growth and regeneration during modified muscle loading in mice in vivo. *J Physiol* 578: 327–336, 2007.
34. **Tsivitse SK, McLoughlin TJ, Peterson JM, Mylona E, McGregor SJ, Pizza FX.** Downhill running in rats: influence on neutrophils, macrophages, and MyoD$^+$ cells in skeletal muscle. *Eur J Appl Physiol* 90: 633–638, 2003.
35. **Warren GL, Lowe DA, Hayes DA, Karwoski CJ, Prior BM, Armstrong RB.** Excitation failure in eccentric contraction-induced injury of mouse soleus muscle. *J Physiol* 468: 487–499, 1993.
36. **West DW, Burd NA, Staples AW, Phillips SM.** Human exercise-mediated skeletal muscle hypertrophy is an intrinsic process. *Int J Biochem Cell Biol* 42: 1371–1375, 2010.
37. **Yablonka-Reuveni Z, Rivera AJ.** Temporal expression of regulatory and structural muscle proteins during myogenesis of satellite cells on isolated adult rat fibers. *Dev Biol* 164: 588–603, 1994.